20 μm cutoff heterojunction interfacial work function internal photoemission detectors

S. G. Matsik,[a] M. B. M. Rinzan, D. G. Esaev, and A. G. U. Perera
Department of Physics and Astronomy, Georgia State University, Atlanta, Georgia 30303

H. C. Liu and M. Buchanan
Institute for Microstructural Sciences, National Research Council, Ottawa, K1A 0R6, Canada

(Received 2 July 2003; accepted 23 October 2003; published online 20 April 2004)

Results are reported on Heterojunction Interfacial Workfunction Internal Photoemission (HEIWIP) detectors designed for operation up to 20 μm. The peak response of 100 mA/W at 12.5 μm with a D^* of 2×10^{11} Jones was observed with a cutoff wavelength of ~20 μm. The BLIP temperature for the devices was 40 K at 1.5 V bias. While the peak response remained almost constant (~95 mA/W) up to 40 K, the D^* reduced to 5×10^{9} Jones due to the increased dark current. The response increased with doping while the dark current did not change significantly. Hence, higher responsivity and D^* can be expected for designs with higher doping. Designs utilizing increased reflection from the bottom contact are suggested to improve the resonant cavity enhancement for optimizing the detectors, which should lead to higher D^* and BLIP temperature. © *2004 American Institute of Physics.* [DOI: 10.1063/1.1634386]

Detectors operating in the 8–20 μm range are attracting increased attention. Recent applications such as the transmission of digital signals using lasers with λ in the range 7–10 μm[1] have been reported. The development of quantum cascade (QC) lasers operating at 21.5 and 24 μm[2] will provide opportunities for extending communication applications to longer wavelengths that will require fast detectors operating at wavelengths longer than the 20 μm currently available[3] with HgCdTe and Quantum Well Infrared Photodetectors (QWIPs). The use of infrared radiation is an important tool for studying astronomy objects with missions such as SOFIA and Herschel (FIRST). The wavelength range up to ~25 μm is particularly useful for studying molecular and dust clouds.[4,5] The direct measurement of temperature and mass density can be obtained from the broadband absorption in dust and spectral lines in molecular hydrogen, water vapor, methane, and other molecules resulting in mapping star formation regions and events like circumstellar shock waves. The wide range of applications in this range makes development of new quantum detectors of an immense interest.

The HEIWIP detection mechanism involves infrared absorption by free carriers in the doped GaAs emitter layers followed by the internal photoemission of photoexcited carriers across the GaAs/$Al_xGa_{1-x}As$ interface and then collection.[6] The structure consists of a sequence of alternating GaAs/AlGaAs layers sandwiched between contact layers. The cutoff wavelength λ_c (μm) is given by 1240/Δ (meV), where Δ is the work-function determined from the energy-gap between the barrier valence band and the emitter Fermi level. The λ_c can be tailored by adjusting the Al fraction.[7] Since the doping is large enough to form a three-dimensional 3-D carrier distribution as opposed to the 2-D distribution of QWIPs, HEIWIPs can be expected to have a lower dark current.[6] Here results are reported on devices with different emitter layer concentrations, specifically designed for operation below 25 μm. The shorter wavelength range should allow an increased Al fraction in the barrier giving a reduced dark current and an increased BLIP temperature compared to the detectors that were reported previously with variable λ_c up to 92 μm.[7]

The HEIWIP structures were grown by Molecular Beam Epitaxy (MBE) on 650 μm-thick semi-insulating GaAs substrates. The structures consist of a 1×10^{19} cm^{-3} Be doped 0.7 μm thick bottom contact, 16 periods of 1250 Å thick $Al_{0.12}Ga_{0.88}As$ undoped barrier/188 Å thick Be-doped GaAs emitter followed by a 1×10^{19} cm^{-3} Be doped 0.2 μm thick top contact. The emitter layer doping was 10, 3, and 1×10^{17} cm^{-3} for samples HE0204, HE0205, and HE0206, respectively. The detectors were fabricated by etching different size mesas using wet etching techniques. Ti/Pt/Au Ohmic contacts were evaporated onto the top and bottom contact layers and a window was opened through the top contact for front side illumination. The top contact was thinned to roughly 1000 Å (with ~100 Å depleted) leaving 900 Å of the top contact to serve as the first emitter layer.

Figure 1(a) shows dark current with bias voltage for HE0204 at various temperatures. These results are consistent with the dominant current mechanism being thermionic emission. Figure 1(b) shows a comparison of dark current at 77 K for the three structures, with sample HE0206 showing a greatly decreased dark current. Samples HE0204 and HE0205 show only a small difference in dark current that is probably related to changes in the bandgap narrowing from the doping. However, due to the same effective barrier height, one expects the same dark current for all three samples. The variation between HE0206 and HE0205 is too large to be explained by bandgap narrowing effects, which should be 1–2 meV at most. It is believed that for the lower doping in HE0206 the impurity and valence bands in the emitter have not yet merged, leading to reduced thermionic current.[8,9] As the doping increases, the upper and lower Hub-

[a]Electronic mail: physgm@panther.gsu.edu

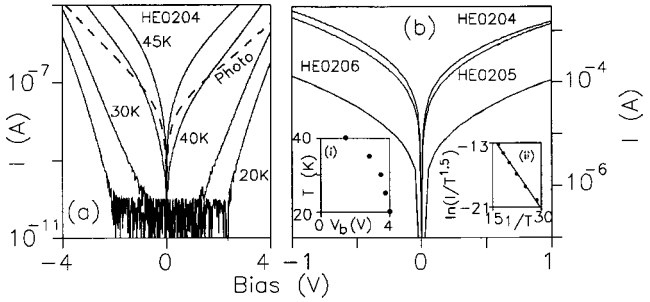

FIG. 1. (a) Plots of dark current vs bias at various temperatures illustrating the thermionic nature of the current. Also shown is the 300 K background photocurrent obtained at 40 K (dashed line). This gives a maximum bias for BLIP behavior of 1.5 V. (b) Dark current at 77 K for the three structures. The doping concentration in the emitters are HE0204, HE0205, and HE0206 are 1×10^{18}, 3×10^{17}, and 1×10^{17}, respectively. Similar variation is observed at 4.2 K, where the currents are lower. Inset i shows the variation of the BLIP temperature with bias voltage. Inset ii shows a modified arrhenious plot of $\ln(I/T^{1.5})$ vs $1/T$ giving an activation energy of $\sim$22 μm.

bard bands increase in width until they merge. At that point the impurity and valence bands merge and the conduction should increase. The differences can be seen clearly at higher temperatures, where the thermionic component is dominant. Also shown in Fig. 1(a) is the 300 K background photocurrent obtained at 40 K showing a BLIP operation for biases $<$1.5 V. As the temperature is decreased the bias for BLIP operation is increased as shown in inset (i) in Fig. 1(b). For temperatures higher than 45 K the dark current was always higher than the photocurrent, and BLIP operation was not possible. A modified arrhenius plot of $\ln(I/T^{3/2})$ vs. $1/T$, shown as inset (ii) to Fig. 1(b), gave an activation energy of $\sim$57 meV ($\lambda_c\sim22$ μm) at a bias of 3.0 V. The activation energy increases as bias decreases, giving 70 meV ($\lambda_c=17.7$ μm) for 1.0 V.

Figure 2(a) shows the measured responsivity in the range 5–20 μm for HE0204 for 4.2–50 K with a peak responsivity of $\sim$0.1 A/W at 12.5 μm for 40 K. The total quantum efficiency determined by dividing the photocurrent by the incident photon rate was $\sim$0.8%. The D^* value calculated from the dark current, assuming full shot noise was 5×10^{10} Jones. The 30% points give a response range of 6–17 μm. The response was relatively stable up to around 40 K, beyond which it decreased, disappearing by $\sim$60 K. The responsivity of the samples with lower doping is greatly reduced, giving

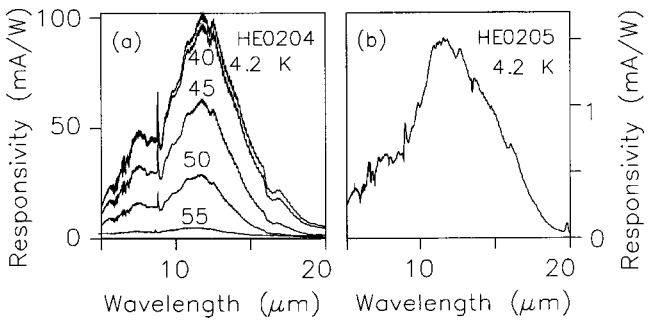

FIG. 2. (a) Measured responsivity of sample HE0204 at various temperatures. The peak response was 0.1 A/W at $\sim$12.5 μm. The response remained constant up to 40 K and then decreased rapidly consistent with the BLIP temperature of 40 K estimated from dark and background current. (b) Responsivity for HE0205 at 4 V bias and 4.2 K showing the greatly reduced response observed when doping is reduced.

TABLE I. Device parameters for the samples used in the measurements. In all cases the emitters were 188 Å GaAs and the barriers were 1250 Å $Al_{0.12}Ga_{0.88}As$ and the contacts were doped to 1×10^{19} cm^{-3}. In all cases $\sim$900 Å (assuming a depletion of $\sim$100 Å) of the top contact were left after etching to form the first emitter. Also shown are the measured values of responsivity and D^*.

Sample	Emitter doping (10^{17} cm^{-3})	Responsivity (mA/W) 4.2 K	D^* (Jones) 4.2 K	D^* (Jones) 40 K
HE0204	10	100	2×10^{11}	5×10^{9}
HE0205	3	1.5	4×10^{9}	
HE0206	1	0.03	4×10^{8}	

1.5 and 0.03 mA/W for HE0205 and HE0206, respectively, at 12.5 μm. The device doping and measured response are listed in Table I. The response at 4.2 K for HE0205 is shown in Fig. 2(b). The responsivity of HE0206 is not shown, as it was greatly reduced. Samples HE0205 and HE0206 showed a response up to temperatures of 50 and 45 K respectively, compared to the 55 K seen for sample HE0204. Although the decreased doping improved the dark current in sample HE0205, the responsivity was reduced drastically, reducing D^*. This indicates that the use of high doping may be the preferable approach. Based on both experimental results and the standard thermionic current calculation, the dark current will not increase significantly as doping is increased until the extremely high doping causes defects in the barrier, which will lead to an increased tunneling current. If the doping is kept below the very high values, the absorption is increased, the response, and hence the BLIP temperature, should increase. From previous experimental response values of 0.5 A/W on FIR ($\lambda_c=70$ μm) detectors[7] with $N_A=3\times10^{18}$ cm^{-3}, it should be possible to increase the doping to at least that level with an expected factor of $\sim$5 gain in responsivity. To avoid increased tunneling from defects at even higher doping, the inclusion of a thin undoped GaAs region between the barrier and emitter could be considered.

The drop in responsivity as the doping is reduced is much larger than expected. Based on theoretical calculations the free carrier absorption should vary as N_A for phonon moderated processes and N_AN_i for impurity moderated processes if the density of ionized impurities is N_i. Since the escape probability does not depend on the doping it is expected that the response should show the same doping dependence as the absorption. N_i is expected to be the same as the hole density N_A, giving a maximum dependence of N_A^2 for the responsivity for the fully ionized impurities. However, based on the experimental results the responsivity varies as $N_A^{3.5}$, which can be explained if the impurities are not fully ionized at low doping levels. This introduces an extra factor that accounts for the observed high dependence of the responsivity on the doping in this regime.

The response can also be enhanced by using the resonant cavity effect.[10] By designing the device for improved reflection from the bottom contact, a resonant cavity can be employed with associated enhancement of the absorption at specific wavelengths. One way to improve reflection is through the use of an *n*- rather than *p*-type bottom contact due to the difference in skin depth and refractive index. Figure 3 shows the calculated absorption in the top emitter for HEIWIP

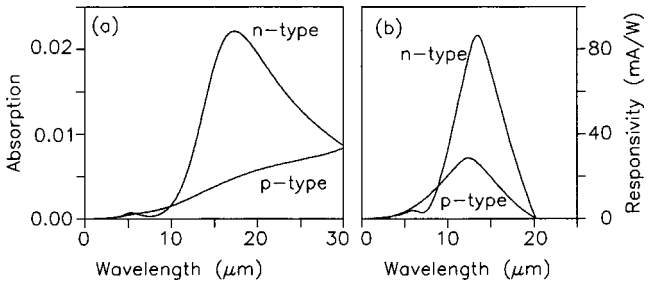

FIG. 3. (a) Plot of calculated absorption in the first emitter (200 Å remainder of the top contact) for devices with *n*- and *p*-type bottom contacts. Both devices had the same parameters as for HE0204, except for a reduced number of periods, to make the λ/4 cavity peak occur near 12 μm. The use of *n*-type material greatly increases the absorption in the 10–20 μm range. (b) The calculated response from the same devices. The use of *n*-type material leads to a factor of 4 increase in the peak response.

structures with a 1×10^{19} cm^{-3} *p*-doped 200 Å thick layer remaining after etching the top contact serving as an effective top emitter, followed by four periods of 1×10^{18} cm^{-3} *p*-doped 188 Å thick GaAs emitters and 1250 Å $Al_{0.12}Ga_{0.88}As$ undoped barriers with a 5000 Å thick bottom contact *p*-doped to 1×10^{19} cm^{-3}. The structures are designed to be similar to the samples used in the measurements with the doping increased and the number of layers reduced to give the λ/4 resonance at ~15 μm. A comparison was made for *n*- and *p*-type doping in the bottom contact. As can be seen, the use of *n*-type doping for the bottom contact will give a much higher absorption at shorter wavelengths than for a *p*-type contact. In addition, the increased skin depth[10] for the *p*-type material leads to optimum absorption at longer wavelengths than are desired for detectors operating below 20 μm. As a result, the *n*-type contact is better at reflecting the radiation below 30 μm. A thicker contact will also increase the reflection for both types of contact as well as shifting the peak absorption to shorter wavelengths in a *p*-type contact. However, there are practical limits on the contact thickness that can be grown. To avoid these limits a doped substrate can be used. The substrate can also serve as the contact region, avoiding the need to include a separate bottom contact in the design.

The modeled response for the structures with *n*- and *p*-type bottom contacts are shown in Fig. 3(b). This gives a response of ~20 mA/W based on just the top emitter compared to the measured peak response of 100 mA/W. The difference is believed to be due to the effects of the other emitters that are not included in the calculation. For an *n*-type bottom contact, based on the calculated curves in Fig. 3, the response would be expected to increase by a factor of 4 to ~400 mA/W. For such a device, assuming the dark current is not increased by the doping so the noise will be similar to HE0204, the predicted BLIP temperature could be ~55 K, with a D^* of 2×10^{10} Jones at the BLIP temperature. By using higher doping (e.g., 3×10^{18} cm^{-3}) the device responsivity can be further increased, giving even higher BLIP temperatures. Future work will concentrate on the use of reflecting bottom contact layers and increased doping to obtain optimized devices.

In conclusion, HEIWIP detectors operating in the 8–20 μm range with a maximum responsivity of 0.1 A/W and $D^*=2\times10^{11}$ Jones at ~12.5 μm and 4.2 K were demonstrated. At 40 K the peak responsivity was 95 mA/W with D^* of 5×10^9 Jones. The BLIP temperature of the detectors was ~40 K and the response was observed up to ~60 K. Although the dark current decreased with decreased emitter doping, the response decreased faster, leading to the device with the highest doping having the best response. With structures optimized for this wavelength range detectors with strong response should be obtainable. The use of resonant cavity effects can be used to increase the response and future work on *n*-type structures should lead to enhanced performance.

This work was supported in part by the National Science Foundation under Grant No. ECS-0140434 and the U.S. Army under Contract No. DAAD19-02-D-0201. M. B. M. Rinzan is supported by GSU RPE funds. The work at NRC is supported in part by DND.

[1] F. Cappaso, R. Paiella, R. Martini *et al.*, IEEE J. Quantum Electron. **38**, 511 (2002).
[2] R. Colombelli, F. Capasso, C. Gmachl, A. L. Hutchinson, D. L. Sivco, A. Tredicucci, M. C. Wanke, A. M. Sergent, and A. Y. Cho, Appl. Phys. Lett. **78**, 2620 (2001).
[3] *Handbook of Thin Film Devices: Semiconductor Optical and Electro Optical Devices*, edited by A. G. U. Perera, H. C. Liu, and M. H. Francombe (Academic, New York, 2001).
[4] P. García-Lario, A. Manchado, A. Ulla, and M. Manteiga, Astrophys. J. **513**, 941 (1999).
[5] S. Deguchi, H. Izumuira, N. Kaifu, X. Mao, N.-Q. Rieu, and N. Ukita, Astron. Astrophys. **315**, L221 (1996).
[6] A. G. U. Perera, S. G. Matsik, B. Yaldiz, H. C. Liu, A. Shen, M. Gao, Z. R. Wasilewski, and M. Buchanan, Appl. Phys. Lett. **78**, 2241 (2001).
[7] S. G. Matsik, M. B. M. Rinzan, A. G. U. Perera, H. C. Liu, Z. R. Wasilewski, and M. Buchanan, Appl. Phys. Lett. **82**, 139 (2003).
[8] Y. N. Yang, D. D. Coon, and P. F. Shepard, Appl. Phys. Lett. **45**, 752 (1984).
[9] A. G. U. Perera, H. X. Yuan, and M. H. Francombe, J. Appl. Phys. **77**, 915 (1995).
[10] D. G. Esaev, S. G. Matsik, M. B. M. Rinzan, A. G. U. Perera, H. C. Liu, and M. Buchanan, J. Appl. Phys. **93**, 1879 (2003).